EXPLORING COMMON HYPERSPECTRAL FEATURES OF EARLY-STAGE PINE WILT DISEASE AT DIFFERENT SCALES, FOR DIFFERENT PINE SPECIES, AND AT DIFFERENT REGIONS

Niwen Li[1,2,3], Langning Huo[3], Xiaoli Zhang[1,2]

[1] Precision Forestry Key Laboratory of Beijing, Forestry College, Beijing Forestry University, Beijing, 100083, China
[2] The Key Laboratory for Silviculture and Conservation of Ministry of Education, Beijing Forestry University, Beijing, 100083, China
[3] Department of Forest Resource Management, Swedish University of Agriculture Sciences, SE-901 83 Umeå, Sweden

ABSTRACT

Pine wilt disease (PWD) is a devastating forest disease and has been listed as a quarantine pest in 52 countries around the world. Early identification of the affected trees and timely removal of them from the forest is crucial to control the spread. This study aims to explore the potential of hyperspectral data on early identification of PWD and exhibit the common spectral features, from early-infected tree crowns and needles, and from different species located in different regions. Two types of hyperspectral data were used and compared. One was using drone-based hyperspectral images with a spectral range of 400 – 1 000 nm and a resolution of 0.11 m. The images were analyzed at the individual-tree level. The other was using hyperspectral reflectance from sampled needles with a spectral range of 350 – 2 500 nm. It was used for the analysis at the needle level. We used linear discriminant analysis (LDA) to quantify the separability of spectral reflectance and first-derivative reflectance from the healthy and early-infected samples. The results showed that the red-edge bands were more sensitive than the other bands at both individual-tree and needle levels, and the first-derivative of red-edge bands achieved the best early recognition of the disease with 0.78, 0.72, and 0.85 accuracy at the individual-tree level for Chinese red pine and at the needle level for Japanese pine and Korean pine. We concluded that red-edge bands were the most informative bands with stable sensitivity at different scales and for different species.

Index Terms— Pine wilt disease, early detection, hyperspectral, drone, classification

1. INTRODUCTION

Pine wilt disease (PWD) is a devastating pine disease caused by pinewood nematodes [1, 2]. It is widely distributed in North America, East Asia, and Europe, causing huge damage to production forests. Pine trees infected with PWD usually die within three months [3]. The nematode cannot travel outside the wood independently but is spread by the main insect vector pine sawyer longhorn-beetles (*Monochamus spp., L.*) during feeding and oviposition [4]. The primary control measure is to cut down and remove the infected trees from the forest as soon as possible to avoid the spread [5], which demands early identification to prevent outbreaks. Yet, research on the early detection of PWD has often been conducted at single scales and with single pine species, and different sensitive bands were proposed and different detection models were used [6,7]. However, the robustness and transferability of the proposed methods have been rarely tested. Therefore, this study focuses on the research questions including (1) what are the common early-infected spectral features observed from different pine species, (2) which spectral features were weakened when upscaling from needle to crown scales, and (3) which wavelengths have stable sensitivities to the early infection among all scales and all species from all regions.

2. MATERIAL

2.1 Study area

The study involves data from three areas. The hyperspectral drone images were acquired in Chaohu City, Anhui Province, China (southeast China, 31°16′—32°N, 117°25′—117°58′E). The area was one of the earliest areas infected by PWD in China. The infected species is mainly Chinese red pine (*Pinus massoniana Lamb.*). The needle samples for the hyperspectral analysis were from Weihai City, Shandong Province (middle-east China, 37°25'~37°25'N, 121°58'~122°17'E) and Fushun City, Liaoning Province (northeast China, 41°14´~42°28´N, 123°39´~125°28´E). The two areas were epidemic areas in 2016 and 2018, and the infected species were Japanese pine (*Pinus densiflora Sieb. et Zucc.*) and Korean pine (*Pinus koraiensis Sieb. et Zucc.*).

2.2 Field data

Field data was collected in November 2019 for the drone-based hyperspectral study. We inventoried trees from 6 plots in 25 m × 25 m squares and recorded the location and health status of individual trees. The field data for the needle-level hyperspectral analysis was conducted in September 2019 in Weihai and August 2020 in Fushun. Needles were collected from sampled trees in 10 and 5 plots in 25 m × 25 m squares in Weihai and Fushun, respectively. In all study areas, the health status of individual trees was estimated according to discoloration (table 1). In Weihai and Fushun, the health status of individual trees was first assessed and sample trees were selected. Needles of the sample trees were cut and collected from four directions of the upper, middle, and lower tree crowns. In this study, we used data from healthy and early-infected trees.

Table 1. Category of the healthy condition and the number of sampled trees.

Infection stage	Color of the tree crowns	Number of trees in Chaohu	Number of trees in Weihai	Number of trees in Fushun
Healthy	Green	50	33	33
Early-stage	less than half of the needles turning yellow, or less than 1/3 of the needles turning red	50	33	25
Middle-stage	more than half of the needles yellow, or the proportion of red needles between 1/3 and 3/4	50	18	10
Late-stage	more than 3/4 needles turning red	50	22	15

2.3 Hyperspectral data acquisition and preprocessing

The hyperspectral drone images were obtained by a Nano-Hyperspec imaging spectrometer system mounted on a DJI Matrice 600 Pro drone. We flew the drone at 120 m above the ground, resulting in a 0.11 m resolution. The wavelength ranged from 400 to 1 000 nm, covering from red band to near-infrared (NIR). The image post-processing included reflectance correction, geometric correction, radiometric correction, and orthorectification. We manually delineated the crowns and averaged the reflectance from individual-tree crowns. We smoothed the spectral curves with a four-point quadratic polynomial Savitzky-Golay filter.

The reflectances from the sampled needles were measured by FiledSpec 4 HR NG spectrometer with a spectral range of 350 nm - 2 500 nm. We measured 10 times for each sample and used the average reflectances. The spectrometer was calibrated every 10 minutes using white reflect panels. The spectral range of 400 - 2 400 nm was used without noise.

3. METHODS

We calculated the separability of the individual bands from healthy and infected trees using linear discriminant analysis (LDA). We randomly selected 80% of samples for training and tested on the remaining 20% of samples, and repeated 100 times of training and testing with random samples. The overall accuracy was calculated to quantify the separability. Similarly, we tested the separability of the first-derivative reflectance.

4. RESULTS AND DISCUSSIONS

In the hyperspectral drone images, red-edge bands showed the highest separability, followed by the green and NIR bands (Figure 1a). The first derivative reflectance at the red-edge band (wavelength 714 nm) showed the highest separability among all bands and achieved an accuracy of 0.78 (Figure 1b).
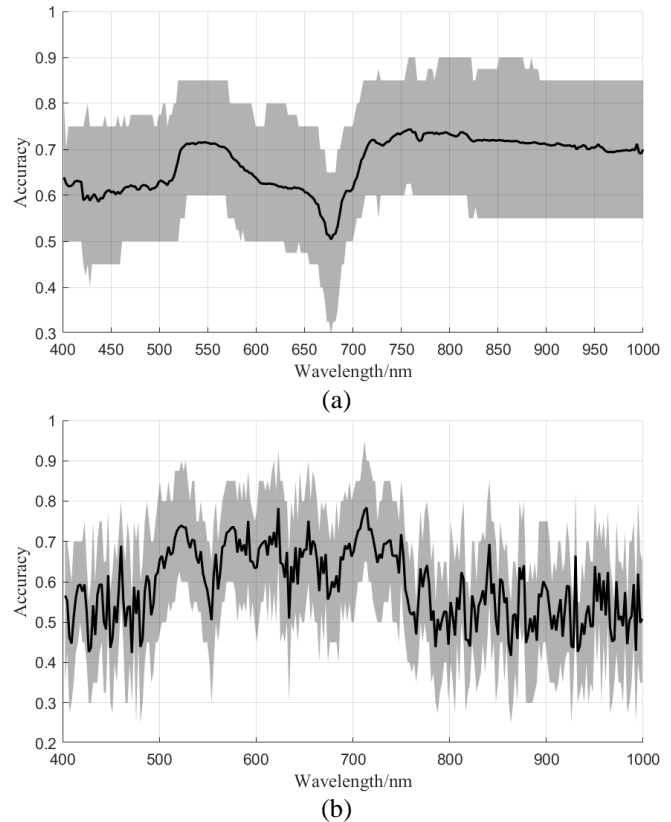

(a)

(b)

Figure 1. The separability of the individual bands of (a) original spectrum and (b) first derivatives spectrum based on hyperspectral drone images. The solid lines are the average separability and the shadows are the 5% - 95% range of the separability.

We measured the hyperspectral reflectance of the needles from two pine species. For both species, the needle reflectances at the red-edge bands showed the highest separability, followed by the NIR, SWIR, and green bands. For Japanese pine, red bands were sensitive to the early infection, but not for Korean pine. For both species, the reflectance showed a peak between 1 600 - 1 800 nm, and the separability at this range was high. For Japanese pine, the reflectance showed a valley around 1 900 nm, and the separability was high. But for Korean pine, the reflectance valley around 1 900 nm was also observed but with low separability between healthy and early-infected trees.

The separability of first-derivative reflectance of the needle samples was high for both species at the ranges 725 - 745 nm, 1 735 - 1 770 nm, 1 840 - 1 847 nm, and 2 049 - 2 066 nm. Especially, the first-derivative reflectance at 729 nm both showed the highest separability compared to other wavelengths for both species. The average overall accuracies in classifying healthy and infected samples were 0.72 and 0.85 for the two pine species using the first-derivative reflectances at 729 nm.

When considering the overall performance of early identification of PWD at different scales, for different pine species, and at different study areas, the first-derivative reflectance at the red-edge bands exhibited the highest capacity to distinguish early-infected trees from healthy trees. At the needle scale, the first-derivative reflectance was most sensitive at 729 nm although samples were collected from different pine species (Japanese and Korean pine) and from different regions (middle-east and northeast China). However, the most sensitive first-derivative reflectance at the crown level was at 714 nm. We propose a hypothesis that the red-edge bands with shorter wavelengths become more sensitive when upscaling. The hypothesis needs to be tested in the future with more multi-scale studies. The reflectance from the red-edges bands also showed the most robust performance among different scales, species, and regions, compared to reflectance from other wavelengths, followed by NIR and green bands. The sensitivity of red bands was not stable for all scales and species. The SWIR bands with 1 600 - 1 800 nm wavelengths were sensitive for both species at the needle level, while their robustness at different scales needs to be tested in future studies.
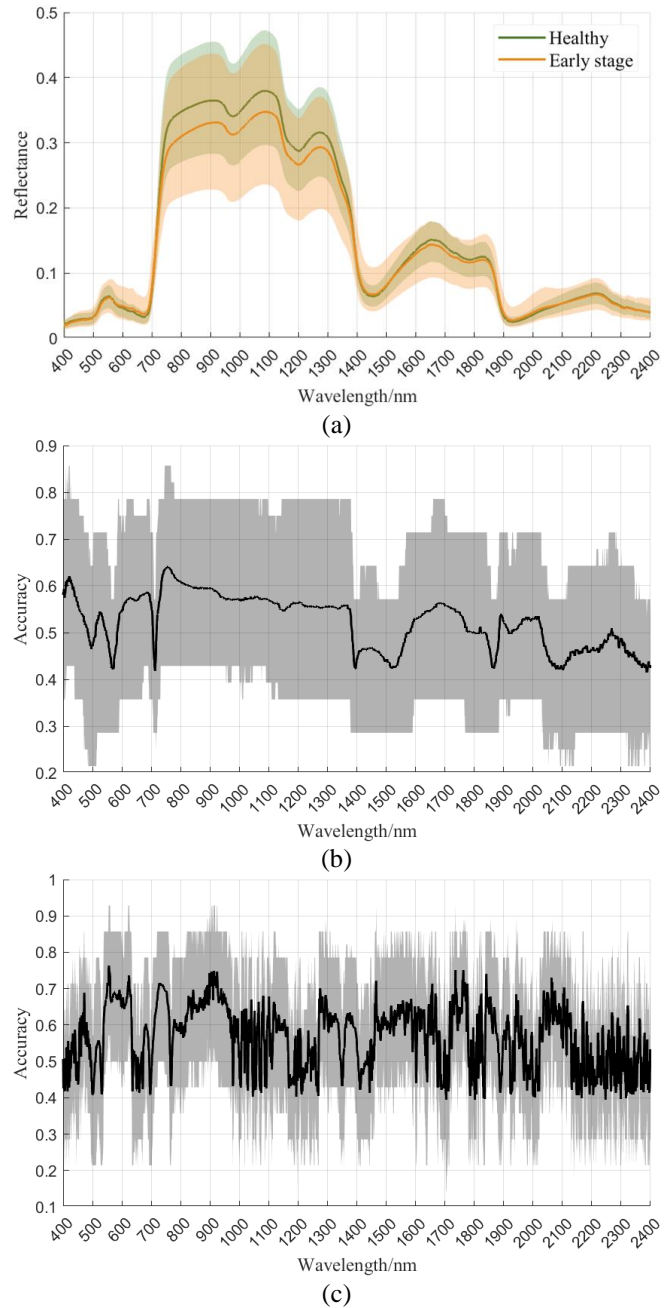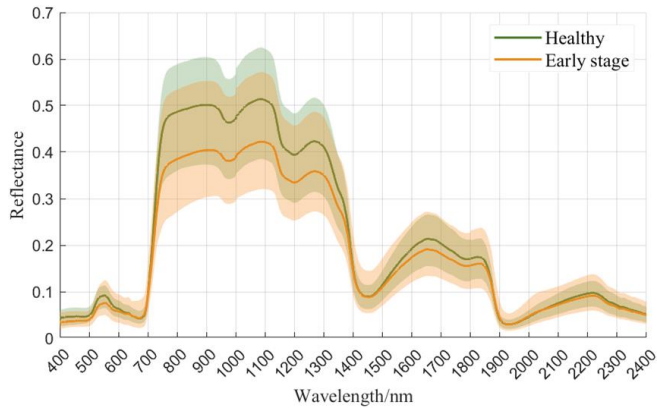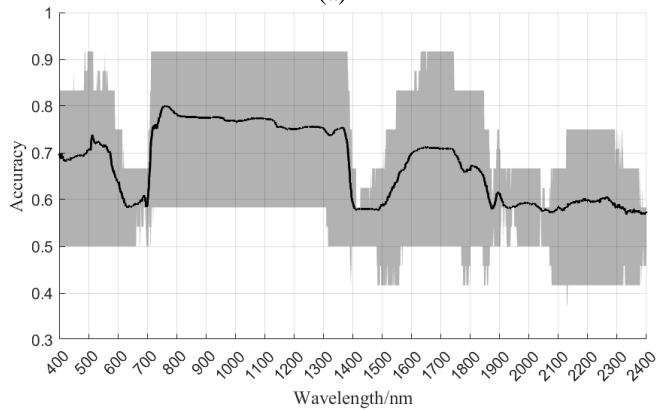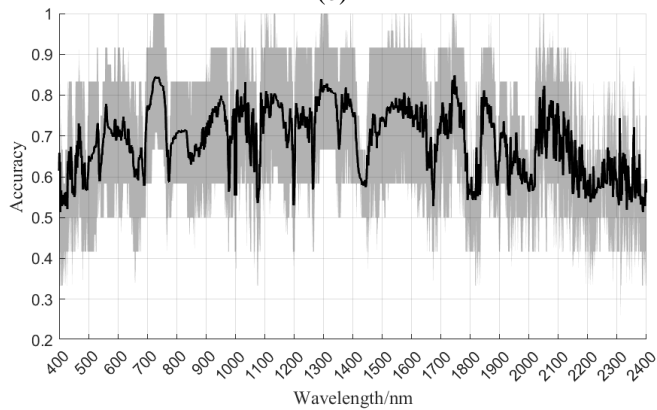

(a)

(b)

(c)

Figure 2. The spectral signatures of healthy and early-infected trees of Japanese pine (a), and the separability of reflectance (b) and first-derivative reflectance (c). The solid lines are the average values and the shadows are the 5% - 95% ranges.

Figure 3. The spectral signatures of healthy and early-infected trees of Korean pine (a), and the separability of reflectance (b) and first-derivative reflectance (c). The solid lines are the average values and the shadows are the 5% - 95% ranges.

5. CONCLUSIONS

This study explored the potential of hyperspectral data in the early identification of PWD at the crown and needle scales, and exhibited the common spectral features observed from different scales, pine species, and regions. We concluded that the first-derivative reflectance from the red-edge bands was most sensitive and robust in the early identification of PWD, followed by the reflectance from the red-edge bands. SWIR bands were sensitive to the early infection for both species at the needle level while their performance was not tested at the crown level in this study.

7. REFERENCES

[1] Sousa, E., Naves, P., & Vieira, M. Prevention of pine wilt disease induced by Bursaphelenchus xylophilus and Monochamus galloprovincialis by trunk injection of emamectin benzoate. Phytoparasitica, 2013, 41: 143-148.

[2] Ikegami, M., & Jenkins, T. Estimate global risks of a forest disease under current and future climates using species distribution model and simple thermal model–Pine Wilt disease as a model case. Forest ecology and management, 2018, 409: 343-352.

[3] Kim, S.R., et al. Hyperspectral analysis of pine wilt disease to determine an optimal detection index. Forests, 2018, 9(3): 115.

[4] Kim, N., et al. Induction of resistance against pine wilt disease caused by Bursaphelenchus xylophilus using selected pine endophytic bacteria. Plant Pathology, 2019, 68(3): 434-444.

[5] Shin, S. C. Pine wilt disease in Korea. Pine wilt disease, 2008: 26-32.

[6] Li, N., Zhang, X., & Huo, L. Identifying Nematode-Induced Wilt Using Hyperspectral Drone Images and Assessing the Potential of Early Detection. IGARSS 2022-2022 IEEE International Geoscience and Remote Sensing Symposium. IEEE, 2022: 512-515.

[7] Li, N., Huo, L., & Zhang, X. Classification of pine wilt disease at different infection stages by diagnostic hyperspectral bands. Ecological Indicators, 2022, 142: 109198.